

## Supporting Online Material for **Mechanism of Na<sup>+</sup>/H<sup>+</sup> Antiporting**

Isaiah T. Arkin, Huafeng Xu, Morten Ø. Jensen, Eyal Arbely, Estelle R. Bennett,  
Kevin J. Bowers, Edmond Chow, Ron O. Dror, Michael P. Eastwood,  
Ravenna Flitman-Tene, Brent A. Gregersen, John L. Klepeis, István Kolossváry,  
Yibing Shan, David E. Shaw\*

\*To whom correspondence should be addressed. E-mail: [david@deshaw.com](mailto:david@deshaw.com)

Published 10 August 2007, *Science* **317**, 799 (2007)

DOI: 10.1126/science.1142824

### This PDF file includes:

Materials and Methods  
SOM Text  
Figs. S1 to S4  
Tables S1 to S4  
References  
Detailed Statement of Software Availability

# Supporting Online Material

## Materials and methods

### Molecular dynamics simulations

#### *Simulation setup*

All simulations used the simple point charge (SPC) model for water (*S1*), the OPLS-AA/L force field for protein (*S2*, *S3*) as provided by the program IMPACT (*S4*, note that the relevant force field option, referred to as OPLS\_2003 in the IMPACT paper, has subsequently been renamed as OPLS\_2005 in the actual program), and standard OPLS parameters for free ions (*S5*, *S6*). Lipid (1-Palmitoyl-2-Oleoyl-sn-Glycero-3-Phosphoethanolamine, POPE) parameters were generated according to protocols consistent with those described in the OPLS literature (*S2*, *S3*, *S7-S12*); on the basis of constant isotropic pressure simulations of the pure POPE bilayer, the lipid acyl chain partial charges were increased to maintain bilayer fluidity (lipid parameters are available in Tables S1-S4).

The simulation system was constructed by embedding the protein, using the X-ray structure (*S13*), in a POPE membrane containing 340 lipids surrounded by 10305 water molecules (*S14*). The lipid bilayer was previously equilibrated at constant pressure ( $P = 1$  bar) and temperature ( $T = 300$ K) resulting in a stable fluid state over 60 ns of MD simulation. The protein was inserted into the bilayer and tilted to maximize hydrophobic matching between protein and lipid. Any lipid and water molecules overlapping the protein were removed, leaving a system with 246 lipid and 10208 water molecules. Appropriate residues (e.g. D78, E82, E124, D133, D163 and D164) were protonated or deprotonated as required by the particular experiment, while protonation states of other residues were set to their default values at pH 7.  $\text{Na}^+$  and  $\text{Cl}^-$  ions were added (by replacing certain water molecules) to neutralize the total charge. The protein was then frozen and the lipids and water were allowed to adhere to it during a short initial NPT ( $P = 1$  bar;  $T = 310$ K) simulation of 0.5 ns. Subsequently, each system was energy-minimized using GROMACS (*S15*).

Each system was equilibrated for 1.2–12 ns at 310 K and 1 bar using Berendsen temperature and pressure control (*S16*). Then a  $\text{Na}^+$ ,  $\text{K}^+$  or  $\text{Li}^+$  ion was introduced in a position appropriate for the particular experiment (i.e., adjacent to the carboxylic group of D163 or D164). After an additional energy minimization step, molecular dynamics simulations were performed under constant temperature and pressure for 12–100 ns. We conducted multiple simulations of  $\text{Na}^+$  transport with different initial random velocities.

#### *Molecular dynamics protocol*

All molecular dynamics simulations were performed using the program Desmond (*S17*) (D. E. Shaw Research, LLC, New York, NY), which uses a particular neutral territory method (*S18*, *S19*) called the midpoint method (*S20*) to efficiently exploit a high degree of computational parallelism. Most simulations ran on 128 dual-processor Opteron nodes (256 processors in total) connected by an Infiniband network (Topspin, San Jose, CA). Long-range electrostatic interactions were

computed by the Gaussian Split Ewald method (GSE) (*S21*) or the Particle Mesh Ewald (PME) method (*S22*). In both cases, we used a  $64 \times 64 \times 64$  Fourier space mesh (mesh spacing  $\leq 1.5$  Å at all times). For GSE, a Gaussian of standard deviation 1.19 Å, truncated at 5.58 Å, was used for charge spreading and force interpolation, while our PME calculations used fourth-order B-splines for interpolation. The real-space part of the electrostatics and the Lennard-Jones interactions were cut off at 10 Å, and a long-range correction was applied to the pressure. Bond lengths to hydrogens were constrained using a variant of M-SHAKE (*S23*). We used a RESPA integrator (*S24*) where the bonded interactions, the Lennard-Jones interactions and the real-space part of the electrostatic interactions were computed every 2 fs, while the Fourier-space electrostatics were computed every 6 fs. The Berendsen pressure and temperature control used relaxation times of 0.5 ps. Equipartition checks were undertaken to ensure that the temperatures of the different components in the systems (i.e. protein, lipid and water) were all at the target temperature ( $T = 310$  K).

### *Free energy perturbation calculations*

The difference in the binding free energies of  $\text{Na}^+$  and  $\text{K}^+$  to NhaA was computed by morphing  $\text{Na}^+$  to  $\text{K}^+$  in (i) water and (ii) the NhaA binding site. The binding free energy difference was calculated as  $\Delta G_{\text{Na}^+}^{\text{binding}} - \Delta G_{\text{K}^+}^{\text{binding}} = \Delta G_{\text{Na}^+ \rightarrow \text{K}^+}^{\text{water}} - \Delta G_{\text{Na}^+ \rightarrow \text{K}^+}^{\text{NhaA}}$ , i.e., the difference in the free energies of morphing  $\text{Na}^+$  to  $\text{K}^+$  in water and in the NhaA binding site (*S25*). The ion's Lennard-Jones interactions were stepped from those of  $\text{Na}^+$  to those of  $\text{K}^+$  over five simulations using the soft-core form (*S26*) of

$$V_{vdW}(r) = \lambda 4\epsilon_{\text{Na}^+} \left( \frac{1}{(\alpha(1-\lambda)^2 + (r/\sigma_{\text{Na}^+})^6)^2} - \frac{1}{\alpha(1-\lambda)^2 + (r/\sigma_{\text{Na}^+})^6} \right) \\ + (1-\lambda) 4\epsilon_{\text{K}^+} \left( \frac{1}{(\alpha\lambda^2 + (r/\sigma_{\text{K}^+})^6)^2} - \frac{1}{\alpha\lambda^2 + (r/\sigma_{\text{K}^+})^6} \right) \quad (I)$$

where  $\alpha = 0.5$ ,  $\lambda$  takes one value from 0, 0.25, 0.5, 0.75, and 1.0 in each of the five simulations, and  $\epsilon_{\text{Na}^+}$ ,  $\epsilon_{\text{K}^+}$ ,  $\sigma_{\text{Na}^+}$ , and  $\sigma_{\text{K}^+}$  are the Lennard-Jones parameters (derived from the original  $\text{Na}^+$  and  $\text{K}^+$  values by geometric combining rules). The Bennett acceptance ratio method (*S27*, *S28*) was used to compute the free energy difference between consecutive  $\lambda$  values. For each  $\lambda$ , the system was first equilibrated for 1 ns, and the potential energy differences were collected every 1.2 ps during the following 5 ns simulation. The data from each simulation were divided into five non-overlapping blocks to yield the free energy difference and its error. An analogous method was used for hydration free energy calculations. The entire procedure was then repeated, substituting  $\text{Li}^+$  for  $\text{K}^+$ .

### *Potential of mean force calculations*

The starting position for each ion-binding simulation was obtained by equilibrating the lipid-embedded NhaA with both D163 and D164 deprotonated, and with the ion vertically (along  $z$ ) constrained to reside 7.5 Å from the ion binding site (at D164) in the direction of the cytoplasm. The membrane plane coincided with the  $xy$  plane of the simulation box (see Fig. S1). The ions ( $\text{Na}^+$ ,  $\text{K}^+$  and  $\text{Li}^+$ ) were each pulled along  $z$  at a rate of  $v = 0.4$  Å/ns, with a spring force constant of  $k = 5$  kcal/mol/Å<sup>2</sup>. Each simulation was conducted in 18 pulling segments and 18 equilibration

steps, each 1.2 ns in length. The potential of mean force (free energy) was computed from the ion trajectories utilizing Jarzynski's identity (S29) as described elsewhere (S30)

$$e^{-\Delta G(\lambda_0 \rightarrow \lambda_1)/k_B T} = \langle e^{-W(\lambda_0 \rightarrow \lambda_1)/k_B T} \rangle \quad (2)$$

The unbiased work ( $W \equiv W(t)$ ) entering the above equation is given by

$$W(t) = W_{ext}(t) - U_B(z, t), \quad U_B(z, t) = \frac{k}{2} (z(t) - z(t=0) - vt)^2 \quad (3)$$

while the external work is given by

$$W_{ext}(t) = -kv \int_0^t dt' [z(t') - z(t'=0) - vt'] \quad (4)$$

The free energy was computed, adopting the stiff spring approximation (S30, S31), by a second-order cumulant expansion (S30) as an average ( $\langle \dots \rangle$ ) over  $N=4$  simulations

$$G(\langle \bar{z}(j) \rangle) = \langle \bar{W}(j) \rangle - (2k_B T)^{-1} \left[ \langle \bar{W}(j)^2 \rangle - \langle \bar{W}(j) \rangle^2 \right] \quad (5)$$

with

$$\langle \bar{W}(j)^2 \rangle = N^{-1} \sum_{n=1}^N \bar{W}_n(j)^2 \text{ and } \langle \bar{z}(j) \rangle = N^{-1} \sum_{n=1}^N \frac{1}{\Delta t} \int_j dt z_n(t). \quad (6)$$

The mean work within the  $j$ th pulling segment of the  $n$ th trajectory ( $\bar{W}_n(j)$ ) was computed as (S30, S31)

$$\bar{W}_n(j) = \Delta t^{-1} \int_j dt [W_{ext,n}(t) - \bar{U}_B(j)] \quad (7)$$

with the biasing potential,  $\bar{U}_B(j)$  given by

$$\bar{U}_B(j) = \frac{k}{2} \left[ \langle \bar{z}(j) \rangle - z(t=0) - \bar{v}t(j) \right]^2, \quad \bar{v}(j) = \Delta t^{-1} \int_j dt t. \quad (8)$$

## Molecular biology experiments

### *Plasmids and bacteria*

The pBR322-derived plasmid containing the *E. coli* antiporter *nhaA* and its regulator *nhaR* (designated pGM36), pBR322, and the *E. coli* strain KNabc (TG1 derivative,  $\Delta nhaA \Delta nhaB \Delta chaA$ ) in which the wt and mutant antiporters were expressed, were all a kind gift from Prof. E. Padan (The Hebrew University of Jerusalem, Israel). Growth experiments in the absence and presence of NaCl were conducted as described previously (S32). In brief, the bacteria were grown at 37 °C in Luria-Bertani (LB) broth or in modified LB broth in which NaCl was replaced by KCl (LBK). Where indicated, NaCl was added and the pH was adjusted to pH 7.0 with 60 mM 1,3 Bis[tris (hydroxymethyl)methylamino]propane (BTP, Sigma). Antibiotics were used in all solid and liquid media as follows: 100 µg/ml ampicillin, 30 µg/ml kanamycin, and 30 µg/ml chloramphenicol.

### *DNA manipulation*

The following mutations of the *nhaA* wild type gene were made: F72A, A100L, G104L, A127L, A160L, F344A, and G336L. Mutation primers were designed using the primer-design software for

QuikChange site-directed mutagenesis and were made using the QuickChange II XL Site-Directed Mutagenesis Kit (Stratagene, La Jolla, CA, USA). A standard PCR protocol was employed (1 min. at 95 °C; 18 cycles consisting of 50 sec. at 95 °C, 50 sec. at 60 °C , and 7 min. 20 sec. at 68 °C; and a termination step of 7 min. at 68 °C ). The mutations were verified by sequencing.

### *nhaA expression*

To express the wild-type and mutant antiporters, KNabc bacteria (*S33*) were transformed with the various constructs using standard transformation protocols. The bacteria were plated on LBK agar, and starters from the transformants were grown overnight in liquid LBK. The cultures were then diluted to an O.D.<sub>600</sub> of 0.02 and grown to an O.D.<sub>600</sub> of 0.6. At this point 10<sup>-1</sup> of each of the cultures were plated on a series of LB agar plates containing 60 mM BTP, pH 7.0, antibiotics, and NaCl at one of the following concentrations: 0.05 M, 0.1 M, 0.2 M, 0.4 M, and 0.6 M. The plates were incubated at 37 °C for 18–24 hours.

## Supporting text

### Mutagenesis data

In addition to the mutations that aimed to probe the accessibility of D163 to protons, we also mutated F72 and F344 to the much smaller residue alanine. Both residues are located at the junction connecting the cytoplasmic Na<sup>+</sup> entry pathway and its periplasmic exit. We hypothesize that these residues help separate the two pathways, preventing the formation of a continuous water file through the protein that might deplete the proton motive force. We find mutation of either residue to be detrimental to the bacteria at higher concentrations of NaCl (Fig. 1C), which is consistent with our hypothesis.

### Free energy perturbation calculations and potential of mean force analyses

The initial conformation of NhaA used in all calculations was that obtained following equilibration for 12 ns with Na<sup>+</sup> occupying the binding site and both D163 and D164 deprotonated. We first calculated the hydration free energies of Li<sup>+</sup> and K<sup>+</sup> relative to that of Na<sup>+</sup>, and then calculated the free energy differences for binding to the protein (results are shown diagrammatically in Fig. S4). As stated in the main text, we find that the protein binds Li<sup>+</sup> more strongly than Na<sup>+</sup> by 16 kJ/mol, and that it binds K<sup>+</sup> more weakly than Na<sup>+</sup> by 14 kJ/mol. Since there is no quantitative experimental data regarding the ion affinities of the antiporter we cannot rigorously assess our predicted results. However, the ion affinity ranking determined computationally agrees with that measured experimentally (*S34, S35*).

The potentials of mean force for Na<sup>+</sup> and Li<sup>+</sup>, computed as a function of the ion's vertical (*z*-axis) position (Fig. S4), indicate that neither of these ions encounter a significant kinetic barrier when approaching D164 from the cytoplasmic vestibule. K<sup>+</sup> did not reach the binding cavity in our simulations but became instead trapped in different local minima. From our free energy perturbation calculations, we conclude that the antiporter favors Na<sup>+</sup> and Li<sup>+</sup> over K<sup>+</sup> thermodynamically, but we do not exclude the possibility that a kinetic component contributes to this selectivity as well.

## Supporting figures

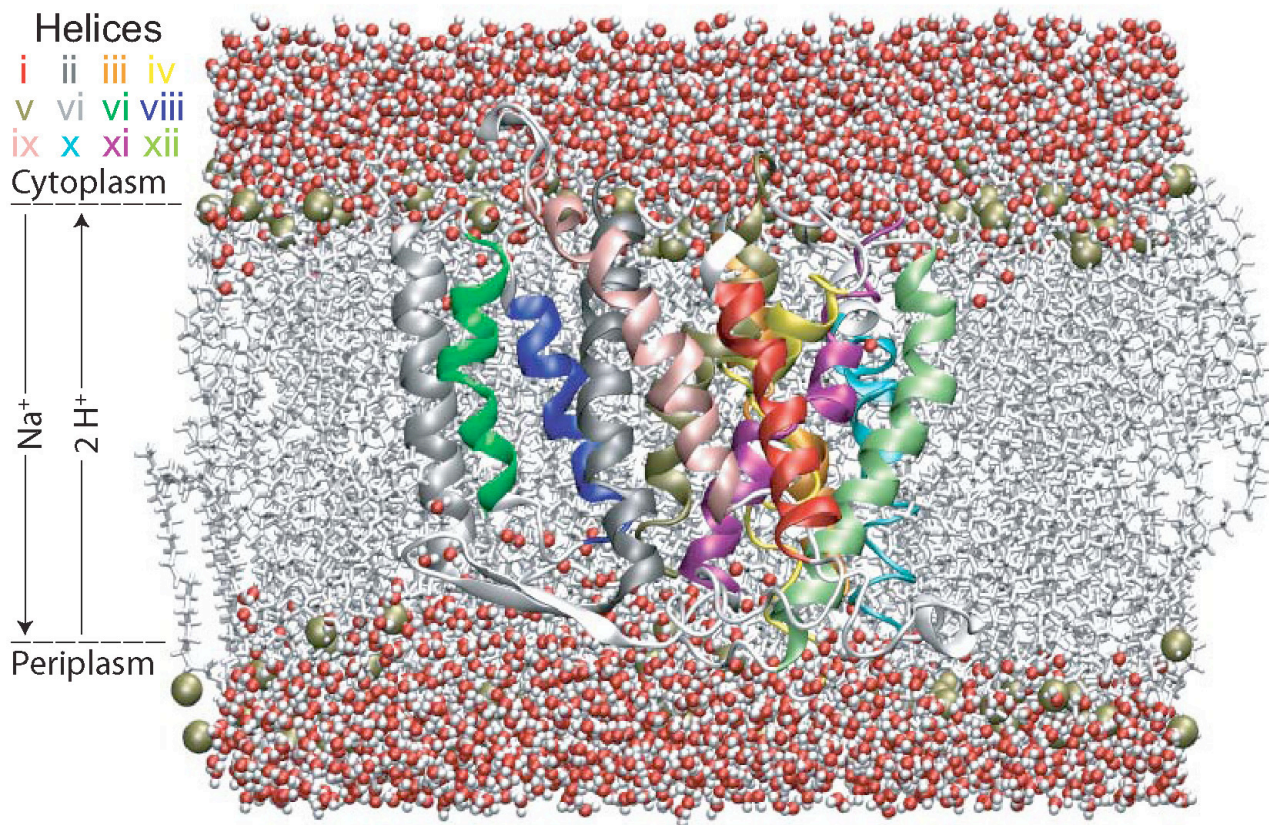


**Figure S1:** Side view of the simulation system. For visual clarity lipid and water molecules that obstructed the view of the protein were removed. The simulation system (ca. 67200 atoms) consisted of the protein, 246 1-Palmitoyl-2-Oleoyl-sn-Glycero-3-Phosphoethanolamine (POPE) lipids, ca. 10200 water molecules, and ca. 5 ions. Helix *i* (residues 12-30) is shown in red, helix *ii* (59-85) in gray, helix *iii* (95-116) in orange, helix *iv* (121-143) in yellow, helix *v* (150-175) in tan, helix *vi* (182-200) in silver, helix *vii* (205-218) in green, helix *viii* (223-236) in blue, helix *ix* (247-271) in pink, helix *x* (290-311) in cyan, helix *xi* (327-350) in purple, and helix *xii* (357-382) in lime. All extra-membrane protein segments are colored in white. Water molecules and lipid phosphates are shown in van der Waals representation, while the remainder of each lipid is shown in white sticks.

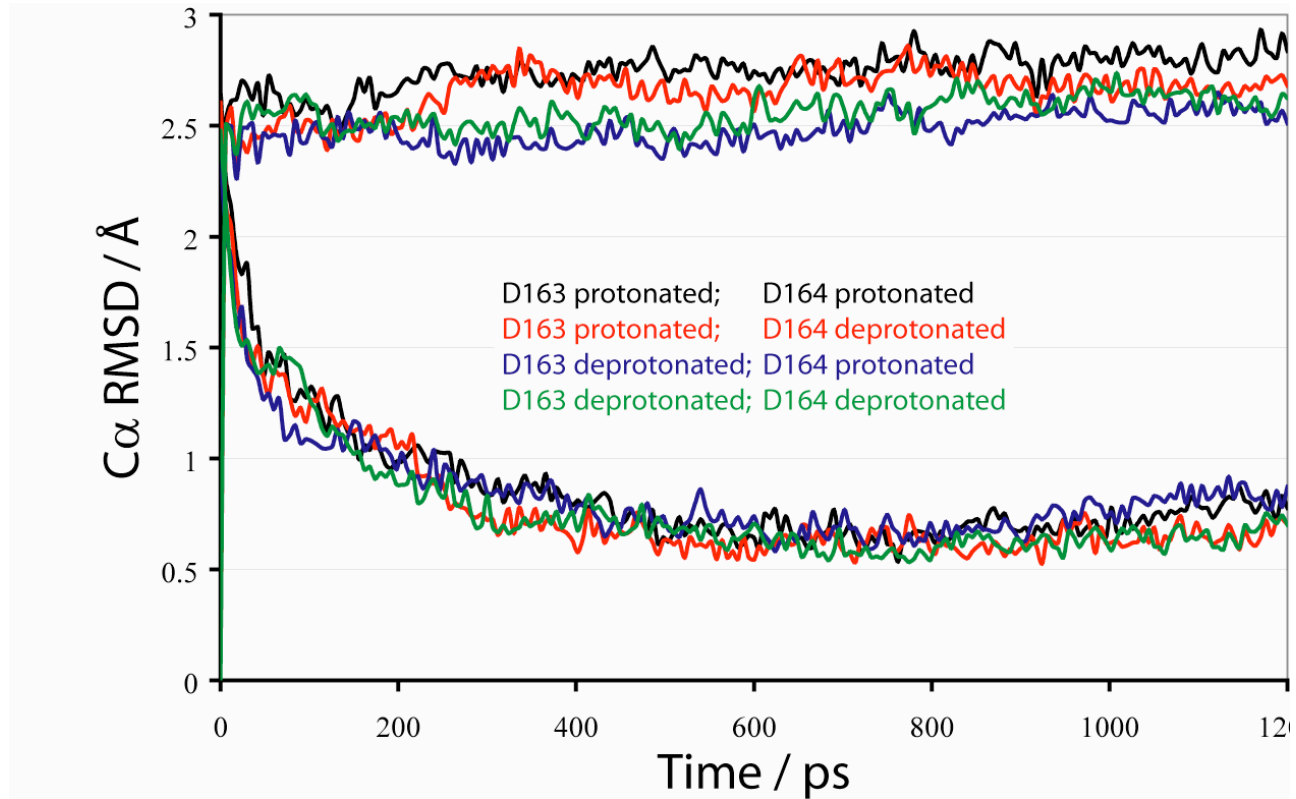
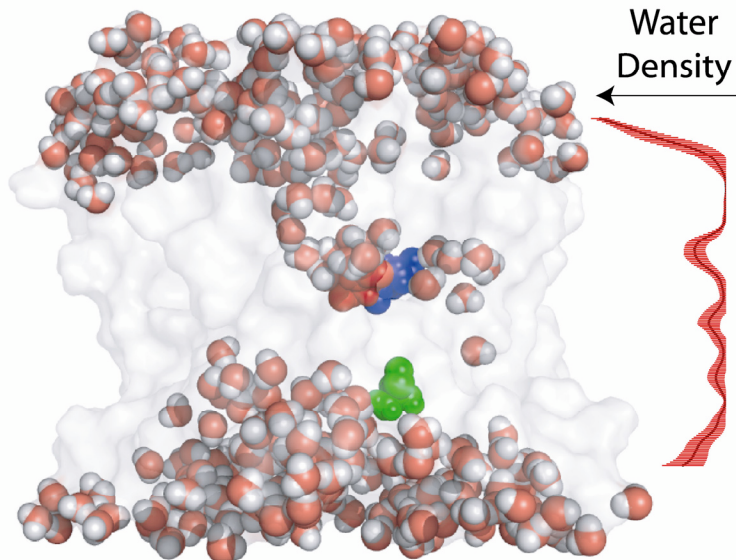


**Figure S2:** C<sub>α</sub> RMSD as a function of equilibration time for the four different starting configurations. The top graphs represent comparisons to the starting configuration (i.e., energy-minimized crystal structure) while the bottom graphs show comparisons to the average structure, obtained by analyzing the last 1 ns of each simulation. The color coding is as follows: black—both D163 and D164 protonated; blue—D163 deprotonated and D164 protonated; red—D163 protonated and D164 deprotonated; green—both D163 and D164 deprotonated. The C<sub>α</sub> RMSD change from the crystal structure was ca. 2.7 Å. After the structures stabilized, they fluctuated around a mean structure with an average C<sub>α</sub> RMSD of ca. 0.7 Å from that mean structure.

WT



A127L

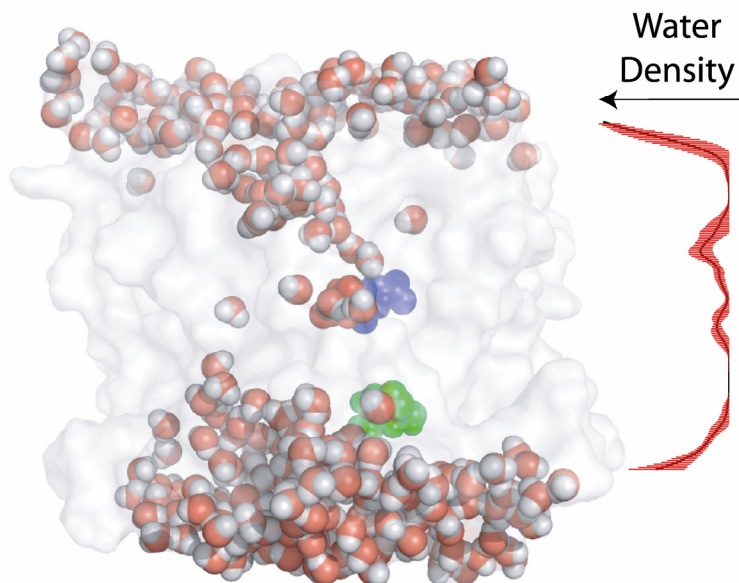


**Figure S3:** Mutagenesis studies of NhaA. Snapshot from simulations of system under mutation of A127L (green), depicting the access pathway of water to D163 (blue). The wild type protein is depicted on top while the mutant is in the bottom panel. D164 is shown in red. The corresponding water densities for the entire simulation are shown on the right of each structure.

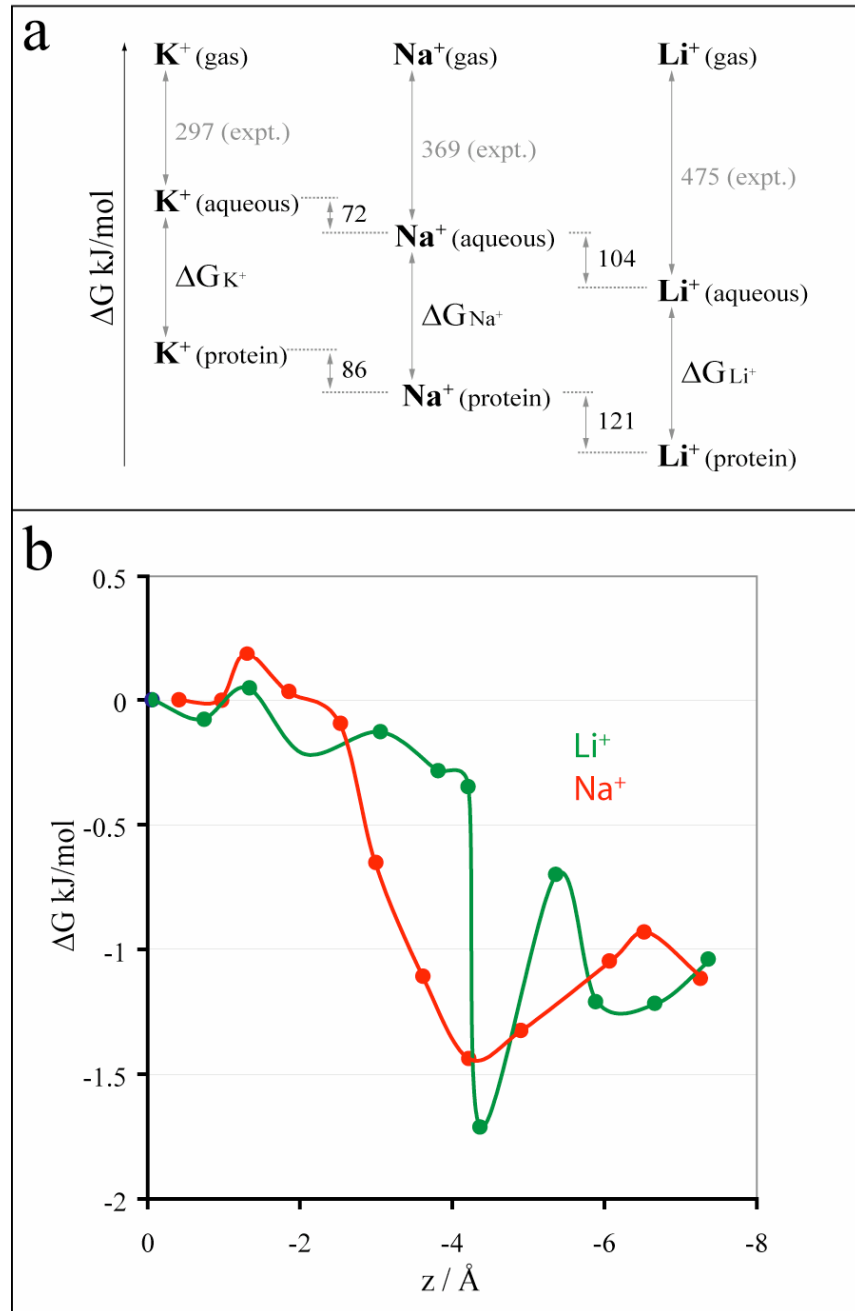


**Figure S4:** Free energy of ion binding. Top panel depicts the free energies, relative to the ions in the gas phase, of the different ions in neat water and bound to the protein. The values in gray are those obtained from experiments (S36-S38), while those in black were calculated in the current study. The bottom panel shows the potential of mean force of  $\text{Na}^+$  in red and  $\text{Li}^+$  in green as a function of the  $z$  coordinate axis, which is perpendicular to the membrane. The ion binding site at D164 is located at  $-7.5 \text{ \AA}$ .

## Supporting tables

**Table S1:** Non-bonded parameters for the POPE lipid. Non-bonded energy is computed as in standard OPLS-AA/L<sup>a</sup>.

Atom #	Atom Name	q <sup>b</sup> , e-	σ <sup>c</sup> , Å	ε <sup>d</sup> , kcal /mol	Atom #	Atom Name	q <sup>b</sup> , e-	σ <sup>c</sup> , Å	ε <sup>d</sup> , kcal /mol	Atom #	Atom Name	q <sup>b</sup> , e-	σ <sup>c</sup> , Å	ε <sup>d</sup> , kcal /mol
1	H1	0.330	0.500	0.030	43	C43	-0.180	3.500	0.066	85	2H30	0.090	2.500	0.030
2	H2	0.330	0.500	0.030	44	C44	-0.180	3.500	0.066	86	1H31	0.090	2.500	0.030
3	H3	0.330	0.500	0.030	45	C45	-0.180	3.500	0.066	87	2H31	0.090	2.500	0.030
4	N4	-0.300	3.250	0.170	46	C46	-0.180	3.500	0.066	88	1H32	0.090	2.420	0.015
5	C5	0.130	3.500	0.066	47	C47	-0.180	3.500	0.066	89	2H32	0.090	2.420	0.015
6	C6	-0.080	3.500	0.066	48	C48	-0.180	3.500	0.066	90	1H36	0.090	2.420	0.015
7	O7	-0.570	2.850	0.140	49	C49	-0.180	3.500	0.066	91	2H36	0.090	2.420	0.015
8	P8	1.500	3.740	0.200	50	C50	-0.270	3.500	0.066	92	1H37	0.090	2.500	0.030
9	O9	-0.780	2.980	0.200	51	CA1	-0.180	3.500	0.066	93	2H37	0.090	2.500	0.030
10	O10	-0.780	2.980	0.200	52	CA2	-0.270	3.500	0.066	94	1H38	0.090	2.500	0.030
11	O11	-0.570	2.850	0.140	53	1H5	0.090	2.500	0.030	95	2H38	0.090	2.500	0.030
12	C12	-0.080	3.500	0.066	54	2H5	0.090	2.500	0.030	96	1H39	0.090	2.500	0.030
13	C13	0.040	3.500	0.066	55	1H6	0.090	2.500	0.030	97	2H39	0.090	2.500	0.030
14	O14	-0.340	3.000	0.170	56	2H6	0.090	2.500	0.030	98	1H40	0.090	2.500	0.030
15	C15	0.630	3.750	0.105	57	1H12	0.090	2.500	0.030	99	2H40	0.090	2.500	0.030
16	O16	-0.520	2.960	0.210	58	2H12	0.090	2.500	0.030	100	1H41	0.090	2.500	0.030
17	C17	-0.080	3.500	0.066	59	H13	0.090	2.420	0.015	101	2H41	0.090	2.500	0.030
18	C18	-0.180	3.500	0.066	60	1H17	0.090	2.420	0.015	102	1H42	0.090	2.500	0.030
19	C19	-0.180	3.500	0.066	61	2H17	0.090	2.420	0.015	103	2H42	0.090	2.500	0.030
20	C20	-0.180	3.500	0.066	62	1H18	0.090	2.500	0.030	104	1H43	0.090	2.500	0.030
21	C21	-0.180	3.500	0.066	63	2H18	0.090	2.500	0.030	105	2H43	0.090	2.500	0.030
22	C22	-0.180	3.500	0.066	64	1H19	0.090	2.500	0.030	106	1H44	0.090	2.500	0.030
23	C23	-0.180	3.500	0.066	65	2H19	0.090	2.500	0.030	107	2H44	0.090	2.500	0.030
24	C24	-0.150	3.550	0.076	66	1H20	0.090	2.500	0.030	108	1H45	0.090	2.500	0.030
25	C25	-0.150	3.550	0.076	67	2H20	0.090	2.500	0.030	109	2H45	0.090	2.500	0.030
26	C26	-0.180	3.500	0.066	68	1H21	0.090	2.500	0.030	110	1H46	0.090	2.500	0.030
27	C27	-0.180	3.500	0.066	69	2H21	0.090	2.500	0.030	111	2H46	0.090	2.500	0.030
28	C28	-0.180	3.500	0.066	70	1H22	0.090	2.500	0.030	112	1H47	0.090	2.500	0.030

29	C29	-0.180	3.500	0.066	71	2H22	0.090	2.500	0.030	113	2H47	0.090	2.500	0.030
30	C30	-0.180	3.500	0.066	72	1H23	0.090	2.500	0.030	114	1H48	0.090	2.500	0.030
31	C31	-0.180	3.500	0.066	73	2H23	0.090	2.500	0.030	115	2H48	0.090	2.500	0.030
32	C32	-0.050	3.500	0.066	74	H24	0.150	2.420	0.030	116	1H49	0.090	2.500	0.030
33	O33	-0.340	3.000	0.170	75	H25	0.150	2.420	0.030	117	2H49	0.090	2.500	0.030
34	C34	0.630	3.750	0.105	76	1H26	0.090	2.500	0.030	118	1H50	0.090	2.500	0.030
35	O35	-0.520	2.960	0.210	77	2H26	0.090	2.500	0.030	119	2H50	0.090	2.500	0.030
36	C36	-0.080	3.500	0.066	78	1H27	0.090	2.500	0.030	120	3H50	0.090	2.500	0.030
37	C37	-0.180	3.500	0.066	79	2H27	0.090	2.500	0.030	121	1HA1	0.090	2.500	0.030
38	C38	-0.180	3.500	0.066	80	1H28	0.090	2.500	0.030	122	2HA1	0.090	2.500	0.030
39	C39	-0.180	3.500	0.066	81	2H28	0.090	2.500	0.030	123	1HA2	0.090	2.500	0.030
40	C40	-0.180	3.500	0.066	82	1H29	0.090	2.500	0.030	124	2HA2	0.090	2.500	0.030
41	C41	-0.180	3.500	0.066	83	2H29	0.090	2.500	0.030	125	3HA2	0.090	2.500	0.030
42	C42	-0.180	3.500	0.066	84	1H30	0.090	2.500	0.030					

<sup>a</sup>  $E_{non-bonded} = \sum_i \sum_{j>i} \left[ \frac{q_i q_j}{r_{ij}} + 4\epsilon_{ij} \left( \left( \frac{\sigma_{ij}}{r_{ij}} \right)^{12} - \left( \frac{\sigma_{ij}}{r_{ij}} \right)^6 \right) \right] f_{ij}$  where  $f_{ij} = 0.5$  if  $ij$  are 1-4; otherwise  $f_{ij} = 1.0$

<sup>b</sup> Charges for acyl chain atoms based on CHARMM values.

<sup>c</sup> Atom based parameters, pair-wise  $\sigma_{ij}$  based on geometric combining rule.

<sup>d</sup> Atom based parameters, pair-wise  $\epsilon_{ij}$  based on geometric combining rule.

**Table S2:** Bond-stretching parameters for the POPE lipid. Bond-stretch energy is computed as in standard OPLS-AA/L<sup>a</sup>.

Atom <i>i</i>	Atom <i>j</i>	$K_r$ , kcal/mol/Å <sup>2</sup>	$r_{eq}$ , Å	Atom <i>i</i>	Atom <i>j</i>	$K_r$ , kcal/mol/Å <sup>2</sup>	$r_{eq}$ , Å	Atom <i>i</i>	Atom <i>j</i>	$K_r$ , kcal/mol/Å <sup>2</sup>	$r_{eq}$ , Å
1	4	868.00	1.010	29	30	536.00	1.529	50	119	680.00	1.090
2	4	868.00	1.010	29	82	680.00	1.090	50	120	680.00	1.090
3	4	868.00	1.010	29	83	680.00	1.090	51	52	536.00	1.529
4	5	734.00	1.471	30	31	536.00	1.529	51	121	680.00	1.090
5	6	536.00	1.529	30	84	680.00	1.090	51	122	680.00	1.090
5	53	680.00	1.090	30	85	680.00	1.090	52	123	680.00	1.090
5	54	680.00	1.090	31	51	536.00	1.529	52	124	680.00	1.090
6	7	640.00	1.410	31	86	680.00	1.090	52	125	680.00	1.090
6	55	680.00	1.090	31	87	680.00	1.090				
6	56	680.00	1.090	32	33	640.00	1.410				
7	8	460.00	1.697	32	88	680.00	1.090				
8	9	1050.00	1.480	32	89	680.00	1.090				
8	10	1050.00	1.480	33	34	428.00	1.327				
8	11	460.00	1.697	34	35	1140.00	1.229				
11	12	640.00	1.410	34	36	634.00	1.522				
12	13	536.00	1.529	36	37	536.00	1.529				
12	57	680.00	1.090	36	90	680.00	1.090				
12	58	680.00	1.090	36	91	680.00	1.090				
13	14	640.00	1.410	37	38	536.00	1.529				
13	32	536.00	1.529	37	92	680.00	1.090				
13	59	680.00	1.090	37	93	680.00	1.090				
14	15	428.00	1.327	38	39	536.00	1.529				
15	16	1140.00	1.229	38	94	680.00	1.090				
15	17	634.00	1.522	38	95	680.00	1.090				
17	18	536.00	1.529	39	40	536.00	1.529				
17	60	680.00	1.090	39	96	680.00	1.090				
17	61	680.00	1.090	39	97	680.00	1.090				

18	19	536.00	1.529	40	41	536.00	1.529			
18	62	680.00	1.090	40	98	680.00	1.090			
18	63	680.00	1.090	40	99	680.00	1.090			
19	20	536.00	1.529	41	42	536.00	1.529			
19	64	680.00	1.090	41	100	680.00	1.090			
19	65	680.00	1.090	41	101	680.00	1.090			
20	21	536.00	1.529	42	43	536.00	1.529			
20	66	680.00	1.090	42	102	680.00	1.090			
20	67	680.00	1.090	42	103	680.00	1.090			
21	22	536.00	1.529	43	44	536.00	1.529			
21	68	680.00	1.090	43	104	680.00	1.090			
21	69	680.00	1.090	43	105	680.00	1.090			
22	23	536.00	1.529	44	45	536.00	1.529			
22	70	680.00	1.090	44	106	680.00	1.090			
22	71	680.00	1.090	44	107	680.00	1.090			
23	24	634.00	1.510	45	46	536.00	1.529			
23	72	680.00	1.090	45	108	680.00	1.090			
23	73	680.00	1.090	45	109	680.00	1.090			
24	25	1098.00	1.340	46	47	536.00	1.529			
24	74	680.00	1.080	46	110	680.00	1.090			
25	26	634.00	1.510	46	111	680.00	1.090			
25	75	680.00	1.080	47	48	536.00	1.529			
26	27	536.00	1.529	47	112	680.00	1.090			
26	76	680.00	1.090	47	113	680.00	1.090			
26	77	680.00	1.090	48	49	536.00	1.529			
27	28	536.00	1.529	48	114	680.00	1.090			
27	78	680.00	1.090	48	115	680.00	1.090			
27	79	680.00	1.090	49	50	536.00	1.529			
28	29	536.00	1.529	49	116	680.00	1.090			
28	80	680.00	1.090	49	117	680.00	1.090			
28	81	680.00	1.090	50	118	680.00	1.090			

$$^aE_{bond} = \sum_{bonds} K_r (r - r_{eq})^2$$

**Table S3:** Angle-bending parameters for the POPE lipid. Angle-bend energy is computed as in standard OPLS-AA/L<sup>a</sup>.

Atom <i>i</i>	Atom <i>j</i>	Atom <i>k</i>	$K_\theta$ , kcal/mol/θ <sup>2</sup>	$\theta_{eq}$ , deg	Atom <i>i</i>	Atom <i>j</i>	Atom <i>k</i>	$K_\theta$ , kcal/mol/θ <sup>2</sup>	$\theta_{eq}$ , deg
1	4	2	70.000	109.500	25	26	27	105.934	109.445
1	4	3	70.000	109.500	25	26	76	70.000	109.500
1	4	5	70.000	109.500	25	26	77	70.000	109.500
2	4	3	70.000	109.500	26	27	28	116.700	112.700
2	4	5	70.000	109.500	26	27	78	75.000	110.700
3	4	5	70.000	109.500	26	27	79	75.000	110.700
4	5	6	160.000	111.200	27	28	29	116.700	112.700
4	5	53	70.000	109.500	27	28	80	75.000	110.700
4	5	54	70.000	109.500	27	28	81	75.000	110.700
5	6	7	100.000	109.500	28	29	30	116.700	112.700
5	6	55	75.000	110.700	28	29	82	75.000	110.700
5	6	56	75.000	110.700	28	29	83	75.000	110.700
6	7	8	200.000	120.500	29	30	31	116.700	112.700
7	8	9	200.000	108.230	29	30	84	75.000	110.700
7	8	10	200.000	108.230	29	30	85	75.000	110.700
7	8	11	90.000	102.600	30	31	51	116.700	112.700
8	11	12	200.000	120.500	30	31	86	75.000	110.700
10	8	9	280.000	119.900	30	31	87	75.000	110.700
11	8	9	200.000	108.230	31	51	52	116.700	112.700
11	8	10	200.000	108.230	31	51	121	75.000	110.700
11	12	13	100.000	109.500	31	51	122	75.000	110.700
11	12	57	70.000	109.500	32	13	14	100.000	109.500
11	12	58	70.000	109.500	32	33	34	166.000	116.900
12	13	14	100.000	109.500	33	34	35	166.000	123.400
12	13	32	116.700	112.700	33	34	36	162.000	111.400
12	13	59	75.000	110.700	34	36	37	126.000	111.100
13	14	15	166.000	116.900	34	36	90	70.000	109.500
13	32	33	100.000	109.500	34	36	91	70.000	109.500

13	32	88	75.000	110.700	36	34	35	160.000	120.400
13	32	89	75.000	110.700	36	37	38	116.700	112.700
14	15	16	166.000	123.400	36	37	92	75.000	110.700
14	15	17	162.000	111.400	36	37	93	75.000	110.700
15	17	18	126.000	111.100	37	38	39	116.700	112.700
15	17	60	70.000	109.500	37	38	94	75.000	110.700
15	17	61	70.000	109.500	37	38	95	75.000	110.700
17	15	16	160.000	120.400	38	39	40	116.700	112.700
17	18	19	116.700	112.700	38	39	96	75.000	110.700
17	18	62	75.000	110.700	38	39	97	75.000	110.700
17	18	63	75.000	110.700	39	40	41	116.700	112.700
18	19	20	116.700	112.700	39	40	98	75.000	110.700
18	19	64	75.000	110.700	39	40	99	75.000	110.700
18	19	65	75.000	110.700	40	41	42	116.700	112.700
19	20	21	116.700	112.700	40	41	100	75.000	110.700
19	20	66	75.000	110.700	40	41	101	75.000	110.700
19	20	67	75.000	110.700	41	42	43	116.700	112.700
20	21	22	116.700	112.700	41	42	102	75.000	110.700
20	21	68	75.000	110.700	41	42	103	75.000	110.700
20	21	69	75.000	110.700	42	43	44	116.700	112.700
21	22	23	116.700	112.700	42	43	104	75.000	110.700
21	22	70	75.000	110.700	42	43	105	75.000	110.700
21	22	71	75.000	110.700	43	44	45	116.700	112.700
22	23	24	105.934	109.445	43	44	106	75.000	110.700
22	23	72	75.000	110.700	43	44	107	75.000	110.700
22	23	73	75.000	110.700	44	45	46	116.700	112.700
23	24	25	140.000	124.000	44	45	108	75.000	110.700
23	24	74	70.000	117.000	44	45	109	75.000	110.700
24	25	26	140.000	124.000	45	46	47	116.700	112.700
24	25	75	70.000	120.000	45	46	110	75.000	110.700

<b>Atom</b>	<b>Atom</b>	<b>Atom</b>	$K_\theta$ ,	$\theta_{eq}$ ,	<b>Atom</b>	<b>Atom</b>	<b>Atom</b>	$K_\theta$ ,	$\theta_{eq}$ ,
<i>i</i>	<i>j</i>	<i>k</i>	kcal/mol/θ <sup>2</sup>	deg	<i>i</i>	<i>j</i>	<i>k</i>	kcal/mol/θ <sup>2</sup>	deg
45	46	111	75.000	110.700	83	29	82	66.000	107.800
46	47	48	116.700	112.700	84	30	31	75.000	110.700
46	47	112	75.000	110.700	85	30	31	75.000	110.700
46	47	113	75.000	110.700	85	30	84	66.000	107.800
47	48	49	116.700	112.700	86	31	51	75.000	110.700
47	48	114	75.000	110.700	87	31	51	75.000	110.700
47	48	115	75.000	110.700	87	31	86	66.000	107.800
48	49	50	116.700	112.700	88	32	33	70.000	109.500
48	49	116	75.000	110.700	89	32	33	70.000	109.500
48	49	117	75.000	110.700	89	32	88	66.000	107.800
49	50	118	75.000	110.700	90	36	37	75.000	110.700
49	50	119	75.000	110.700	91	36	37	75.000	110.700
49	50	120	75.000	110.700	91	36	90	66.000	107.800
51	52	123	75.000	110.700	92	37	38	75.000	110.700
51	52	124	75.000	110.700	93	37	38	75.000	110.700
51	52	125	75.000	110.700	93	37	92	66.000	107.800
53	5	6	75.000	110.700	94	38	39	75.000	110.700
54	5	6	75.000	110.700	95	38	39	75.000	110.700
54	5	53	66.000	107.800	95	38	94	66.000	107.800
55	6	7	70.000	109.500	96	39	40	75.000	110.700
56	6	7	70.000	109.500	97	39	40	75.000	110.700
56	6	55	66.000	107.800	97	39	96	66.000	107.800
57	12	13	75.000	110.700	98	40	41	75.000	110.700
58	12	13	75.000	110.700	99	40	41	75.000	110.700
58	12	57	66.000	107.800	99	40	98	66.000	107.800
59	13	14	70.000	109.500	100	41	42	75.000	110.700
59	13	32	75.000	110.700	101	41	42	75.000	110.700
60	17	18	75.000	110.700	101	41	100	66.000	107.800
61	17	18	75.000	110.700	102	42	43	75.000	110.700
61	17	60	66.000	107.800	103	42	43	75.000	110.700
62	18	19	75.000	110.700	103	42	102	66.000	107.800
63	18	19	75.000	110.700	104	43	44	75.000	110.700

63	18	62		66.000	107.800	105	43	44		75.000	110.700
64	19	20		75.000	110.700	105	43	104		66.000	107.800
65	19	20		75.000	110.700	106	44	45		75.000	110.700
65	19	64		66.000	107.800	107	44	45		75.000	110.700
66	20	21		75.000	110.700	107	44	106		66.000	107.800
67	20	21		75.000	110.700	108	45	46		75.000	110.700
67	20	66		66.000	107.800	109	45	46		75.000	110.700
68	21	22		75.000	110.700	109	45	108		66.000	107.800
69	21	22		75.000	110.700	110	46	47		75.000	110.700
69	21	68		66.000	107.800	111	46	47		75.000	110.700
70	22	23		75.000	110.700	111	46	110		66.000	107.800
71	22	23		75.000	110.700	112	47	48		75.000	110.700
71	22	70		66.000	107.800	113	47	48		75.000	110.700
72	23	24		70.000	109.500	113	47	112		66.000	107.800
73	23	24		70.000	109.500	114	48	49		75.000	110.700
73	23	72		66.000	107.800	115	48	49		75.000	110.700
74	24	25		70.000	120.000	115	48	114		66.000	107.800
75	25	26		70.000	117.000	116	49	50		75.000	110.700
76	26	27		75.000	110.700	117	49	50		75.000	110.700
77	26	27		75.000	110.700	117	49	116		66.000	107.800
77	26	76		66.000	107.800	119	50	118		66.000	107.800
78	27	28		75.000	110.700	120	50	118		66.000	107.800
79	27	28		75.000	110.700	120	50	119		66.000	107.800
79	27	78		66.000	107.800	121	51	52		75.000	110.700
80	28	29		75.000	110.700	122	51	52		75.000	110.700
81	28	29		75.000	110.700	122	51	121		66.000	107.800
81	28	80		66.000	107.800	124	52	123		66.000	107.800
82	29	30		75.000	110.700	125	52	123		66.000	107.800
83	29	30		75.000	110.700	125	52	124		66.000	107.800

$$^a E_{angle} = \sum_{angles} K_\theta (\theta - \theta_{eq})^2$$

**Table S4:** Torsional parameters for the POPE lipid. Torsional energy is computed as in standard OPLS-AA/L<sup>a</sup>.

Atom <i>i</i>	Atom <i>j</i>	Atom <i>k</i>	Atom <i>l</i>	<i>V</i> <sub>1</sub> , kcal/mol	<i>V</i> <sub>2</sub> , kcal/mol	<i>V</i> <sub>3</sub> , kcal/mol	Atom <i>i</i>	Atom <i>j</i>	Atom <i>k</i>	Atom <i>l</i>	<i>V</i> <sub>1</sub> , kcal/mol	<i>V</i> <sub>2</sub> , kcal/mol	<i>V</i> <sub>3</sub> , kcal/mol
1	4	5	6	0.000	0.000	0.347	21	22	23	73	0.000	0.000	0.300
1	4	5	53	0.000	0.000	0.261	22	23	24	25	-0.046	2.895	-1.052
1	4	5	54	0.000	0.000	0.261	22	23	24	74	0.000	-2.399	0.000
2	4	5	6	0.000	0.000	0.347	23	24	25	26	0.000	14.000	0.000
2	4	5	53	0.000	0.000	0.261	23	24	25	75	0.000	14.000	0.000
2	4	5	54	0.000	0.000	0.261	24	25	26	27	-0.046	2.895	-1.052
3	4	5	6	0.000	0.000	0.347	24	25	26	76	0.000	0.000	0.000
3	4	5	53	0.000	0.000	0.261	24	25	26	77	0.000	0.000	0.000
3	4	5	54	0.000	0.000	0.261	25	26	27	28	0.301	0.180	0.906
4	5	6	7	2.307	0.475	0.267	25	26	27	78	0.000	0.000	-0.020
4	5	6	55	0.000	0.000	0.384	25	26	27	79	0.000	0.000	-0.020
4	5	6	56	0.000	0.000	0.384	26	27	28	29	0.483	0.432	0.544
5	6	7	8	-5.109	-0.407	0.380	26	27	28	80	0.000	0.000	0.300
6	7	8	9	0.027	0.459	-0.012	26	27	28	81	0.000	0.000	0.300
6	7	8	10	0.027	0.459	-0.012	27	28	29	30	0.483	0.432	0.544
6	7	8	11	0.081	-2.181	1.417	27	28	29	82	0.000	0.000	0.300
7	8	11	12	0.081	-2.181	1.417	27	28	29	83	0.000	0.000	0.300
8	11	12	13	-5.109	-0.407	0.380	28	29	30	31	0.483	0.432	0.544
8	11	12	57	0.000	0.000	0.030	28	29	30	84	0.000	0.000	0.300
8	11	12	58	0.000	0.000	0.030	28	29	30	85	0.000	0.000	0.300
9	8	11	12	0.027	0.459	-0.012	29	30	31	51	0.483	0.432	0.544
10	8	11	12	0.027	0.459	-0.012	29	30	31	86	0.000	0.000	0.300
11	12	13	14	2.307	-2.368	-0.436	29	30	31	87	0.000	0.000	0.300
11	12	13	32	1.017	-0.468	0.820	30	31	51	52	0.483	0.432	0.544
11	12	13	59	0.000	0.000	0.390	30	31	51	121	0.000	0.000	0.300
12	13	14	15	-0.436	-0.915	0.283	30	31	51	122	0.000	0.000	0.300
12	13	32	33	1.017	-0.468	0.820	31	51	52	123	0.000	0.000	0.300
12	13	32	88	0.000	0.000	0.300	31	51	52	124	0.000	0.000	0.300
12	13	32	89	0.000	0.000	0.300	31	51	52	125	0.000	0.000	0.300
13	14	15	16	0.000	12.627	0.000	32	13	14	15	-0.436	-0.915	0.283

13	14	15	17	3.466	-1.001	0.000	32	33	34	35	0.000	12.627	0.000
13	32	33	34	-0.436	-0.915	0.283	32	33	34	36	3.466	-1.001	0.000
14	13	32	33	2.307	-2.368	-0.436	33	34	36	37	0.000	0.000	-0.370
14	13	32	88	0.000	0.000	0.390	33	34	36	90	0.000	0.000	0.065
14	13	32	89	0.000	0.000	0.390	33	34	36	91	0.000	0.000	0.065
14	15	17	18	0.000	0.000	-0.370	34	36	37	38	-2.007	0.387	1.002
14	15	17	60	0.000	0.000	0.065	34	36	37	92	0.000	0.000	-0.111
14	15	17	61	0.000	0.000	0.065	34	36	37	93	0.000	0.000	-0.111
15	17	18	19	-2.007	0.387	1.002	35	34	36	37	-0.409	0.808	-0.563
15	17	18	62	0.000	0.000	-0.111	35	34	36	90	0.000	0.000	0.000
15	17	18	63	0.000	0.000	-0.111	35	34	36	91	0.000	0.000	0.000
16	15	17	18	-0.409	0.808	-0.563	36	37	38	39	0.483	0.432	0.544
16	15	17	60	0.000	0.000	0.000	36	37	38	94	0.000	0.000	0.300
16	15	17	61	0.000	0.000	0.000	36	37	38	95	0.000	0.000	0.300
17	18	19	20	0.483	0.432	0.544	37	38	39	40	0.483	0.432	0.544
17	18	19	64	0.000	0.000	0.300	37	38	39	96	0.000	0.000	0.300
17	18	19	65	0.000	0.000	0.300	37	38	39	97	0.000	0.000	0.300
18	19	20	21	0.483	0.432	0.544	38	39	40	41	0.483	0.432	0.544
18	19	20	66	0.000	0.000	0.300	38	39	40	98	0.000	0.000	0.300
18	19	20	67	0.000	0.000	0.300	38	39	40	99	0.000	0.000	0.300
19	20	21	22	0.483	0.432	0.544	39	40	41	42	0.483	0.432	0.544
19	20	21	68	0.000	0.000	0.300	39	40	41	100	0.000	0.000	0.300
19	20	21	69	0.000	0.000	0.300	39	40	41	101	0.000	0.000	0.300
20	21	22	23	0.483	0.432	0.544	40	41	42	43	0.483	0.432	0.544
20	21	22	70	0.000	0.000	0.300	40	41	42	102	0.000	0.000	0.300
20	21	22	71	0.000	0.000	0.300	40	41	42	103	0.000	0.000	0.300
21	22	23	24	0.301	0.180	0.906	41	42	43	44	0.483	0.432	0.544
21	22	23	72	0.000	0.000	0.300	41	42	43	104	0.000	0.000	0.300

<b>Atom</b>	<b>Atom</b>	<b>Atom</b>	<b>Atom</b>	$V_1,$ <b>kcal/mol</b>	$V_2,$ <b>kcal/mol</b>	$V_3,$ <b>kcal/mol</b>	<b>Atom</b>	<b>Atom</b>	<b>Atom</b>	<b>Atom</b>	$V_1,$ <b>kcal/mol</b>	$V_2,$ <b>kcal/mol</b>	$V_3,$ <b>kcal/mol</b>
<i>i</i>	<i>j</i>	<i>k</i>	<i>l</i>				<i>i</i>	<i>j</i>	<i>k</i>	<i>l</i>			
41	42	43	105	0.000	0.000	0.300	66	20	21	22	0.000	0.000	0.300
42	43	44	45	0.483	0.432	0.544	66	20	21	68	0.000	0.000	0.300
42	43	44	106	0.000	0.000	0.300	66	20	21	69	0.000	0.000	0.300
42	43	44	107	0.000	0.000	0.300	67	20	21	22	0.000	0.000	0.300
43	44	45	46	0.483	0.432	0.544	67	20	21	68	0.000	0.000	0.300
43	44	45	108	0.000	0.000	0.300	67	20	21	69	0.000	0.000	0.300
43	44	45	109	0.000	0.000	0.300	68	21	22	23	0.000	0.000	0.300
44	45	46	47	0.483	0.432	0.544	68	21	22	70	0.000	0.000	0.300
44	45	46	110	0.000	0.000	0.300	68	21	22	71	0.000	0.000	0.300
44	45	46	111	0.000	0.000	0.300	69	21	22	23	0.000	0.000	0.300
45	46	47	48	0.483	0.432	0.544	69	21	22	70	0.000	0.000	0.300
45	46	47	112	0.000	0.000	0.300	69	21	22	71	0.000	0.000	0.300
45	46	47	113	0.000	0.000	0.300	70	22	23	24	0.000	0.000	-0.020
46	47	48	49	0.483	0.432	0.544	70	22	23	72	0.000	0.000	0.300
46	47	48	114	0.000	0.000	0.300	70	22	23	73	0.000	0.000	0.300
46	47	48	115	0.000	0.000	0.300	71	22	23	24	0.000	0.000	-0.020
47	48	49	50	0.483	0.432	0.544	71	22	23	72	0.000	0.000	0.300
47	48	49	116	0.000	0.000	0.300	71	22	23	73	0.000	0.000	0.300
47	48	49	117	0.000	0.000	0.300	72	23	24	25	0.000	0.000	0.000
48	49	50	118	0.000	0.000	0.300	72	23	24	74	0.000	0.000	0.656
48	49	50	119	0.000	0.000	0.300	73	23	24	25	0.000	0.000	0.000
48	49	50	120	0.000	0.000	0.300	73	23	24	74	0.000	0.000	0.656
53	5	6	7	0.000	0.000	0.390	74	24	25	26	0.000	14.000	0.000
53	5	6	55	0.000	0.000	0.300	74	24	25	75	0.000	14.000	0.000
53	5	6	56	0.000	0.000	0.300	75	25	26	27	0.000	-2.399	0.000
54	5	6	7	0.000	0.000	0.390	75	25	26	76	0.000	0.000	0.656
54	5	6	55	0.000	0.000	0.300	75	25	26	77	0.000	0.000	0.656
54	5	6	56	0.000	0.000	0.300	76	26	27	28	0.000	0.000	0.300
55	6	7	8	0.000	0.000	0.030	76	26	27	78	0.000	0.000	0.300
56	6	7	8	0.000	0.000	0.030	76	26	27	79	0.000	0.000	0.300
57	12	13	14	0.000	0.000	0.390	77	26	27	28	0.000	0.000	0.300
57	12	13	32	0.000	0.000	0.300	77	26	27	78	0.000	0.000	0.300

57	12	13	59	0.000	0.000	0.300	77	26	27	79	0.000	0.000	0.300
58	12	13	14	0.000	0.000	0.390	78	27	28	29	0.000	0.000	0.300
58	12	13	32	0.000	0.000	0.300	78	27	28	80	0.000	0.000	0.300
58	12	13	59	0.000	0.000	0.300	78	27	28	81	0.000	0.000	0.300
59	13	14	15	0.000	0.000	0.102	79	27	28	29	0.000	0.000	0.300
59	13	32	33	0.000	0.000	0.390	79	27	28	80	0.000	0.000	0.300
59	13	32	88	0.000	0.000	0.300	79	27	28	81	0.000	0.000	0.300
59	13	32	89	0.000	0.000	0.300	80	28	29	30	0.000	0.000	0.300
60	17	18	19	0.000	0.000	0.300	80	28	29	82	0.000	0.000	0.300
60	17	18	62	0.000	0.000	0.300	80	28	29	83	0.000	0.000	0.300
60	17	18	63	0.000	0.000	0.300	81	28	29	30	0.000	0.000	0.300
61	17	18	19	0.000	0.000	0.300	81	28	29	82	0.000	0.000	0.300
61	17	18	62	0.000	0.000	0.300	81	28	29	83	0.000	0.000	0.300
61	17	18	63	0.000	0.000	0.300	82	29	30	31	0.000	0.000	0.300
62	18	19	20	0.000	0.000	0.300	82	29	30	84	0.000	0.000	0.300
62	18	19	64	0.000	0.000	0.300	82	29	30	85	0.000	0.000	0.300
62	18	19	65	0.000	0.000	0.300	83	29	30	31	0.000	0.000	0.300
63	18	19	20	0.000	0.000	0.300	83	29	30	84	0.000	0.000	0.300
63	18	19	64	0.000	0.000	0.300	83	29	30	85	0.000	0.000	0.300
63	18	19	65	0.000	0.000	0.300	84	30	31	51	0.000	0.000	0.300
64	19	20	21	0.000	0.000	0.300	84	30	31	86	0.000	0.000	0.300
64	19	20	66	0.000	0.000	0.300	84	30	31	87	0.000	0.000	0.300
64	19	20	67	0.000	0.000	0.300	85	30	31	51	0.000	0.000	0.300
65	19	20	21	0.000	0.000	0.300	85	30	31	86	0.000	0.000	0.300
65	19	20	66	0.000	0.000	0.300	85	30	31	87	0.000	0.000	0.300
65	19	20	67	0.000	0.000	0.300	86	31	51	52	0.000	0.000	0.300

<b>Atom</b>	<b>Atom</b>	<b>Atom</b>	<b>Atom</b>	<b><math>V_1,</math></b>	<b><math>V_2,</math></b>	<b><math>V_3,</math></b>	<b>Atom</b>	<b>Atom</b>	<b>Atom</b>	<b>Atom</b>	<b><math>V_1,</math></b>	<b><math>V_2,</math></b>	<b><math>V_3,</math></b>
<i>i</i>	<i>j</i>	<i>k</i>	<i>l</i>	<b>kcal/mol</b>	<b>kcal/mol</b>	<b>kcal/mol</b>	<i>i</i>	<i>j</i>	<i>k</i>	<i>l</i>	<b>kcal/mol</b>	<b>kcal/mol</b>	<b>kcal/mol</b>
86	31	51	121	0.000	0.000	0.300	107	44	45	46	0.000	0.000	0.300
86	31	51	122	0.000	0.000	0.300	107	44	45	108	0.000	0.000	0.300
87	31	51	52	0.000	0.000	0.300	107	44	45	109	0.000	0.000	0.300
87	31	51	121	0.000	0.000	0.300	108	45	46	47	0.000	0.000	0.300
87	31	51	122	0.000	0.000	0.300	108	45	46	110	0.000	0.000	0.300
88	32	33	34	0.000	0.000	0.102	108	45	46	111	0.000	0.000	0.300
89	32	33	34	0.000	0.000	0.102	109	45	46	47	0.000	0.000	0.300
90	36	37	38	0.000	0.000	0.300	109	45	46	110	0.000	0.000	0.300
90	36	37	92	0.000	0.000	0.300	109	45	46	111	0.000	0.000	0.300
90	36	37	93	0.000	0.000	0.300	110	46	47	48	0.000	0.000	0.300
91	36	37	38	0.000	0.000	0.300	110	46	47	112	0.000	0.000	0.300
91	36	37	92	0.000	0.000	0.300	110	46	47	113	0.000	0.000	0.300
91	36	37	93	0.000	0.000	0.300	111	46	47	48	0.000	0.000	0.300
92	37	38	39	0.000	0.000	0.300	111	46	47	112	0.000	0.000	0.300
92	37	38	94	0.000	0.000	0.300	111	46	47	113	0.000	0.000	0.300
92	37	38	95	0.000	0.000	0.300	112	47	48	49	0.000	0.000	0.300
93	37	38	39	0.000	0.000	0.300	112	47	48	114	0.000	0.000	0.300
93	37	38	94	0.000	0.000	0.300	112	47	48	115	0.000	0.000	0.300
93	37	38	95	0.000	0.000	0.300	113	47	48	49	0.000	0.000	0.300
94	38	39	40	0.000	0.000	0.300	113	47	48	114	0.000	0.000	0.300
94	38	39	96	0.000	0.000	0.300	113	47	48	115	0.000	0.000	0.300
94	38	39	97	0.000	0.000	0.300	114	48	49	50	0.000	0.000	0.300
95	38	39	40	0.000	0.000	0.300	114	48	49	116	0.000	0.000	0.300
95	38	39	96	0.000	0.000	0.300	114	48	49	117	0.000	0.000	0.300
95	38	39	97	0.000	0.000	0.300	115	48	49	50	0.000	0.000	0.300
96	39	40	41	0.000	0.000	0.300	115	48	49	116	0.000	0.000	0.300
96	39	40	98	0.000	0.000	0.300	115	48	49	117	0.000	0.000	0.300
96	39	40	99	0.000	0.000	0.300	116	49	50	118	0.000	0.000	0.300
97	39	40	41	0.000	0.000	0.300	116	49	50	119	0.000	0.000	0.300
97	39	40	98	0.000	0.000	0.300	116	49	50	120	0.000	0.000	0.300
97	39	40	99	0.000	0.000	0.300	117	49	50	118	0.000	0.000	0.300
98	40	41	42	0.000	0.000	0.300	117	49	50	119	0.000	0.000	0.300

98	40	41	100	0.000	0.000	0.300	117	49	50	120	0.000	0.000	0.300
98	40	41	101	0.000	0.000	0.300	121	51	52	123	0.000	0.000	0.300
99	40	41	42	0.000	0.000	0.300	121	51	52	124	0.000	0.000	0.300
99	40	41	100	0.000	0.000	0.300	121	51	52	125	0.000	0.000	0.300
99	40	41	101	0.000	0.000	0.300	122	51	52	123	0.000	0.000	0.300
100	41	42	43	0.000	0.000	0.300	122	51	52	124	0.000	0.000	0.300
100	41	42	102	0.000	0.000	0.300	122	51	52	125	0.000	0.000	0.300
100	41	42	103	0.000	0.000	0.300	14	17	15	16	0.000	21.000	0.000
101	41	42	43	0.000	0.000	0.300	23	74	24	25	0.000	30.000	0.000
101	41	42	102	0.000	0.000	0.300	26	75	25	24	0.000	30.000	0.000
101	41	42	103	0.000	0.000	0.300	33	36	34	35	0.000	21.000	0.000
102	42	43	44	0.000	0.000	0.300							
102	42	43	104	0.000	0.000	0.300							
102	42	43	105	0.000	0.000	0.300							
103	42	43	44	0.000	0.000	0.300							
103	42	43	104	0.000	0.000	0.300							
103	42	43	105	0.000	0.000	0.300							
104	43	44	45	0.000	0.000	0.300							
104	43	44	106	0.000	0.000	0.300							
104	43	44	107	0.000	0.000	0.300							
105	43	44	45	0.000	0.000	0.300							
105	43	44	106	0.000	0.000	0.300							
105	43	44	107	0.000	0.000	0.300							
106	44	45	46	0.000	0.000	0.300							
106	44	45	108	0.000	0.000	0.300							
106	44	45	109	0.000	0.000	0.300							

$$^a E_{torsion} = \frac{V_1}{2} [1 + \cos(\phi)] + \frac{V_2}{2} [1 - \cos(2\phi)] + \frac{V_3}{2} [1 + \cos(3\phi)]$$

## Supporting references

- S1. H. J. C. Berendsen, J. P. M. Postma, W. F. van Gunsteren, J. Hermans, in *Intermolecular Forces*, B. Pullman, Ed. (D. Reidel Publishing Company, Dordrecht, 1981) pp. 331-342.
- S2. G. A. Kaminski, R. A. Friesner, J. Tirado-Rives, W. L. Jorgensen, *J Phys Chem B* **105**, 6474 (2001).
- S3. M. P. Jacobson, G. A. Kaminski, R. A. Friesner, *J Phys Chem B* **106**, 11673 (2002).
- S4. J. L. Banks *et al.*, *J Comput Chem* **26**, 1752 (2005).
- S5. J. Aqvist, *J Phys Chem* **94**, 8021 (1990).
- S6. W. L. Jorgensen, J. P. Ulmschneider, J. Tirado-Rives, *J Phys Chem B* **108**, 16264 (2004).
- S7. W. Damm, A. Frontera, J. Tirado-Rives, W. L. Jorgensen, *J Comp Chem* **18**, 1955 (1997).
- S8. W. L. Jorgensen, D. S. Maxwell, J. Tirado-Rives, *J Am Chem Soc* **118**, 11225 (1996).
- S9. W. L. Jorgensen, N. A. McDonald, *Theochem-J Mol Struc* **424**, 145 (1998).
- S10. N. A. McDonald, W. L. Jorgensen, *J Phys Chem B* **102**, 8049 (1998).
- S11. R. C. Rizzo, W. L. Jorgensen, *J Am Chem Soc* **121**, 4827 (1999).
- S12. E. K. Watkins, W. L. Jorgensen, *J Phys Chem A* **105**, 4118 (2001).
- S13. C. Hunte *et al.*, *Nature* **435**, 1197 (2005).
- S14. D. P. Tieleman, H. J. Berendsen, *Biophys J* **74**, 2786 (1998).
- S15. D. van der Spoel *et al.*, *J Comput Chem* **26**, 1701 (2005).
- S16. H. J. C. Berendsen, J. P. M. Postma, W. F. van Gunsteren, A. Dinola, J. R. Haak, *J Chem Phys* **81**, 3684 (1984).
- S17. K. J. Bowers *et al.*, in Proceedings of the ACM/IEEE Conference on Supercomputing 2006 (SC06), Tampa, Florida (2006).
- S18. D. E. Shaw, *J Comput Chem* **26**, 1318 (2005).
- S19. K. J. Bowers, R. O. Dror, D. E. Shaw, *J Comput Phys* **221**, 303 (2007).
- S20. K. J. Bowers, R. O. Dror, D. E. Shaw, *J Chem Phys* **124**, 184109 (2006).
- S21. Y. Shan, J. L. Klepeis, M. P. Eastwood, R. O. Dror, D. E. Shaw, *J Chem Phys* **122**, 54101 (2005).
- S22. T. Darden, D. York, L. Pedersen, *J Chem Phys* **98**, 10089 (1993).
- S23. V. Krautler, W. F. van Gunsteren, P. H. Hunenberger, *J Comput Chem* **22**, 501 (2001).
- S24. M. Tuckerman, B. J. Berne, G. J. Martyna, *J Chem Phys* **97**, 1990 (1992).
- S25. P. Kollman, *Chem Rev* **93**, 2395 (1993).
- S26. T. C. Beutler, A. E. Mark, R. C. van Schaik, P. R. Gerber, W. F. van Gunsteren, *Chem Phys Lett* **222**, 529 (1994).
- S27. C. H. Bennett, *J Comp Phys* **22**, 245 (1976).
- S28. M. R. Shirts, E. Bair, G. Hooker, V. S. Pande, *Phys Rev Lett* **91** (2003).
- S29. C. Jarzynski, *Phys Rev Lett* **78**, 2690 (1997).
- S30. M. O. Jensen, S. Park, E. Tajkhorshid, K. Schulten, *Proc Natl Acad Sci USA* **99**, 6731 (2002).
- S31. S. Park, K. Schulten, *J Chem Phys* **120**, 5946 (2004).
- S32. K. Herz, S. Vimont, E. Padan, P. Berche, *J Bacteriol* **185**, 1236 (2003).
- S33. K. Nozaki, K. Inaba, T. Kuroda, M. Tsuda, T. Tsuchiya, *Biochem Biophys Res Commun* **222**, 774 (1996).
- S34. E. Padan, N. Maisler, D. Taglicht, R. Karpel, S. Schuldiner, *J Biol Chem* **264**, 20297 (1989).

- S35. D. Zuber *et al.*, *Biochim Biophys Acta* **1709**, 240 (2005).
- S36. B. E. Conway, *J Sol Chem* **7**, 721 (1978).
- S37. H. L. K. Friedman, C. V. Krishnan, in *Water: A Comprehensive Treatise*, F. Franks, Ed. (Plenum, New York, 1973), vol. 3, pp. 1-118.
- S38. Y. Marcus, *J Chem Soc, Faraday Trans* **87**, 2995 (1991).

## Detailed Statement of Software Availability

The first version of Desmond designed for use by external researchers is scheduled for release by the end of 2007. This version will be available for purchase by commercial users from Schrödinger LLC, and will also be made available without cost by D. E. Shaw Research for non-commercial research use by universities and other not-for-profit institutions. (If the number of such non-commercial research users ultimately grows to the point where the associated costs become significant, however, D. E. Shaw Research may begin charging such users a fee in order to cover these costs.) During the period prior to this first external release, the authors are prepared to make the *current* version of Desmond available upon request to any reader of Science (either directly or through Schrödinger, as described above). The current version, however, does not include various usability features that are expected to be included in the externally released version, and may thus be more difficult to use without assistance and support from the authors. Because of the limited resources available for such assistance and support, the authors reserve the right to give priority to those researchers who are interested in assessing or better understanding the results described in this article, and to ask some or all (depending on resource availability) other users to wait for the release of the first external version.